PERGAMON

Journal of Structural Geology 24 (2002) 1587–1602

JOURNAL OF STRUCTURAL GEOLOGY

www.elsevier.com/locate/jstrugeo

Crossing the several scales of strain-accomplishing mechanisms in the hinterland of the central Andean fold–thrust belt, Bolivia

Nadine McQuarrie[a,b,*], George H. Davis[a]

[a]Department of Geosciences, University of Arizona, Tucson, AZ 85721, USA
[b]Division of Geological and Planetary Science, California Institute of Technology, Pasadena, CA 91125, USA

Received 14 November 2000; revised 28 October 2001; accepted 29 October 2001

Abstract

Depictions of structures at outcrop, regional and tectonic scales enforce horizontal shortening and vertical thickening as the predominant style of deformation at all scales within the hinterland of the central Andean fold–thrust belt. Outcrop-scale structures document a progression of strain that created: (1) flexural-slip folds, (2) fold flattening via axial-planar cleavage, (3) vertical stretching via boudinage and late-stage faulting and, finally, (4) kink folding. These examples of intraformational deformation are generally concentrated just beyond the tip lines of thrust faults, where fault-propagation folds and related structures are well developed. Fault-propagation folding accommodated the accrual of strain indicated by outcrop-scale structures while the structures themselves indicate how deformation developed within each individual fold. Fault-propagation fold geometries at a regional scale emerge from the construction of regional balanced cross-sections. The sections were drawn with careful attention to: (1) known map relationships, (2) field inspection of key contacts, (3) bedding–orientation data, (4) local seismic control, and (5) principles of balance. The pervasive ESE–WNW shortening and vertical elongation seen at the outcrop and regional scales developed during the formation of the central Andean backthrust belt in the hinterland of the Andes. The central Andean backthrust belt is a large-scale west-vergent thrust system along the western side of the Eastern Cordillera in the generally east-vergent Andean fold–thrust belt of Bolivia. Strain accrual within this west-verging zone of deformation is proposed to be a taper-building mechanism that allowed the fold–thrust belt to continue propagating eastward. © 2002 Published by Elsevier Science Ltd.

Keywords: Fold–thrust belt; Strain; Bolivian Andes; Deformation processes

1. Introduction

Depictions of structural or tectonic mechanisms typically are scale dependent. The coarse nature of regional cross-sections prevents capturing the details of strain and deformation seen in outcrop-scale structures throughout the line of section. By focusing on structures unique to one particular scale, differences arise with respect to the dominant mechanisms of deformation. It is commonly difficult to reconcile seemingly pervasive outcrop-scale deformation with regional cross-sections showing homoclinally dipping panels of rocks separated by discrete faults. A more complete picture can be achieved through an integration of several different scales ranging from outcrop to tectonic (e.g. Mitra and Elliott, 1980; Mitra et al., 1984; Mitra, 1987; Boyer and Mitra, 1988; Gray and Mitra, 1993). This permits more comprehensive understanding of what the structures have in common kinematically. In the central Andes these commonalities are vertical stretching and horizontal shortening of individual folds and of the fold–thrust belt as a whole. The purpose of this contribution is to describe intraformational deformational processes and structures produced at magnitudes too small to be portrayed on regional structural sections, and then to integrate these observations with regional structures as portrayed in the balanced cross-section. By keying diagnostic outcrop-scale structures to their structural positions in a regional cross-section, we can establish a progressive deformational history that is consistent with structures seen at all scales. Understanding intraformational structural styles and deformation mechanisms elucidates the progressive and incremental nature of the thin-skinned folding and thrusting.

2. Geologic setting

2.1. Regional background

The area of focus for this paper is within the hinterland of

* Corresponding author. Present address: Division of Geological and Planetary Science, California Institute of Technology MC 100-23, Pasadena, CA 91125, USA. Tel.: +1-626-395-6486; fax: +1-626-683-0621.
E-mail address: nmcq@gps.caltech.edu (N. McQuarrie).

0191-8141/02/$ - see front matter © 2002 Published by Elsevier Science Ltd.
PII: S0191-8141(01)00158-4

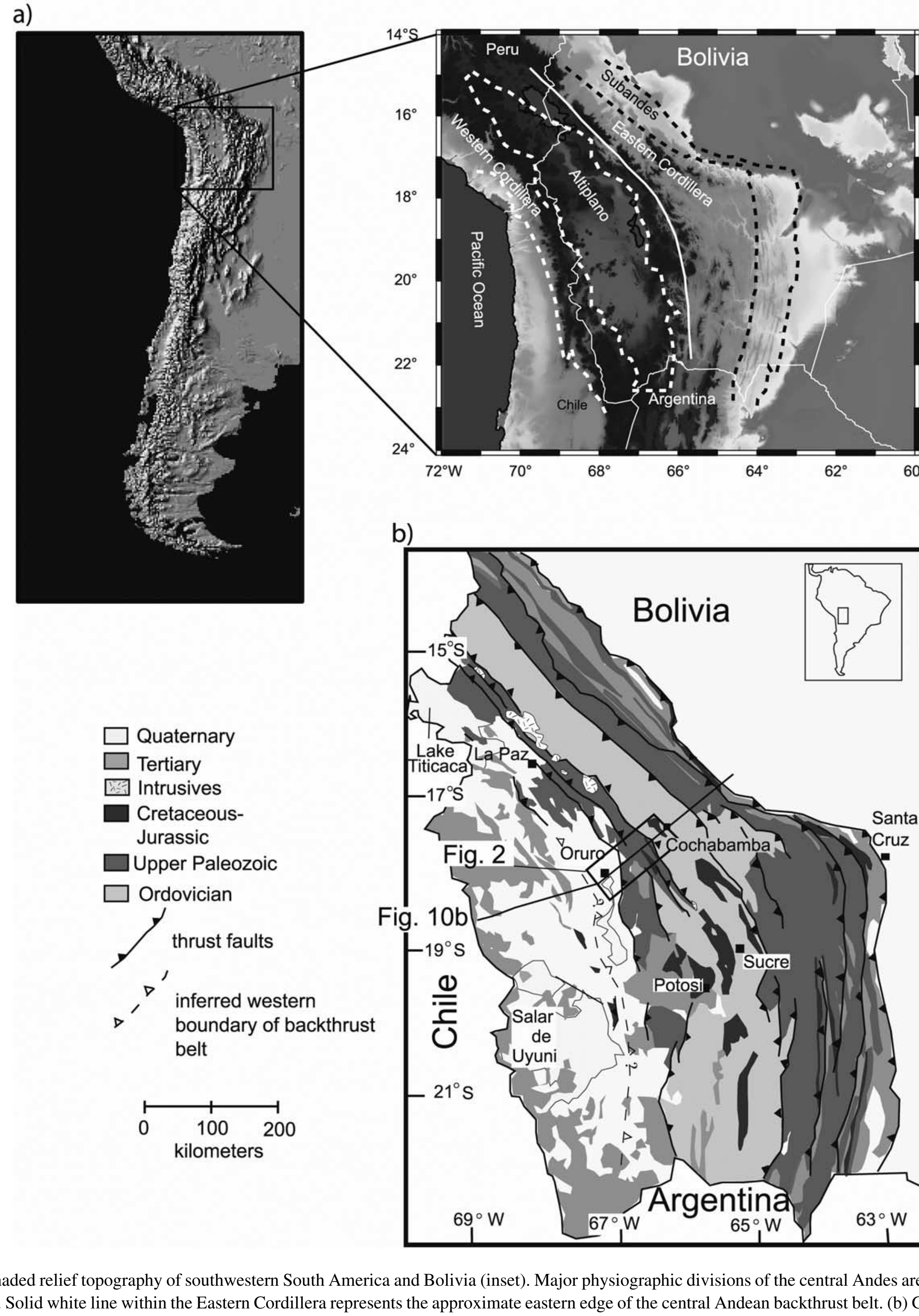

Fig. 1. (a) Shaded relief topography of southwestern South America and Bolivia (inset). Major physiographic divisions of the central Andes are highlighted by dashed lines. Solid white line within the Eastern Cordillera represents the approximate eastern edge of the central Andean backthrust belt. (b) Geologic map of Bolivia (simplified from Pareja et al. (1978)) illustrating major lithologic boundaries, thrust systems, and locations of regional maps and cross-sections. Geographic extent of the Central Andean backthrust belt is indicated by the thrust faults with open barbs on their east side.

the central Andean fold–thrust belt located in Bolivia. The central Andean fold–thrust belt is part of the Andean mountain chain, which extends ~8000 km along the western margin of South America and is the result of shortening associated with the subduction of the Nazca Plate (Fig. 1a). The central Andes in northern Chile and Bolivia form the widest portion of the mountain belt and contain a 400-km-wide orogenic plateau in the hinterland of the

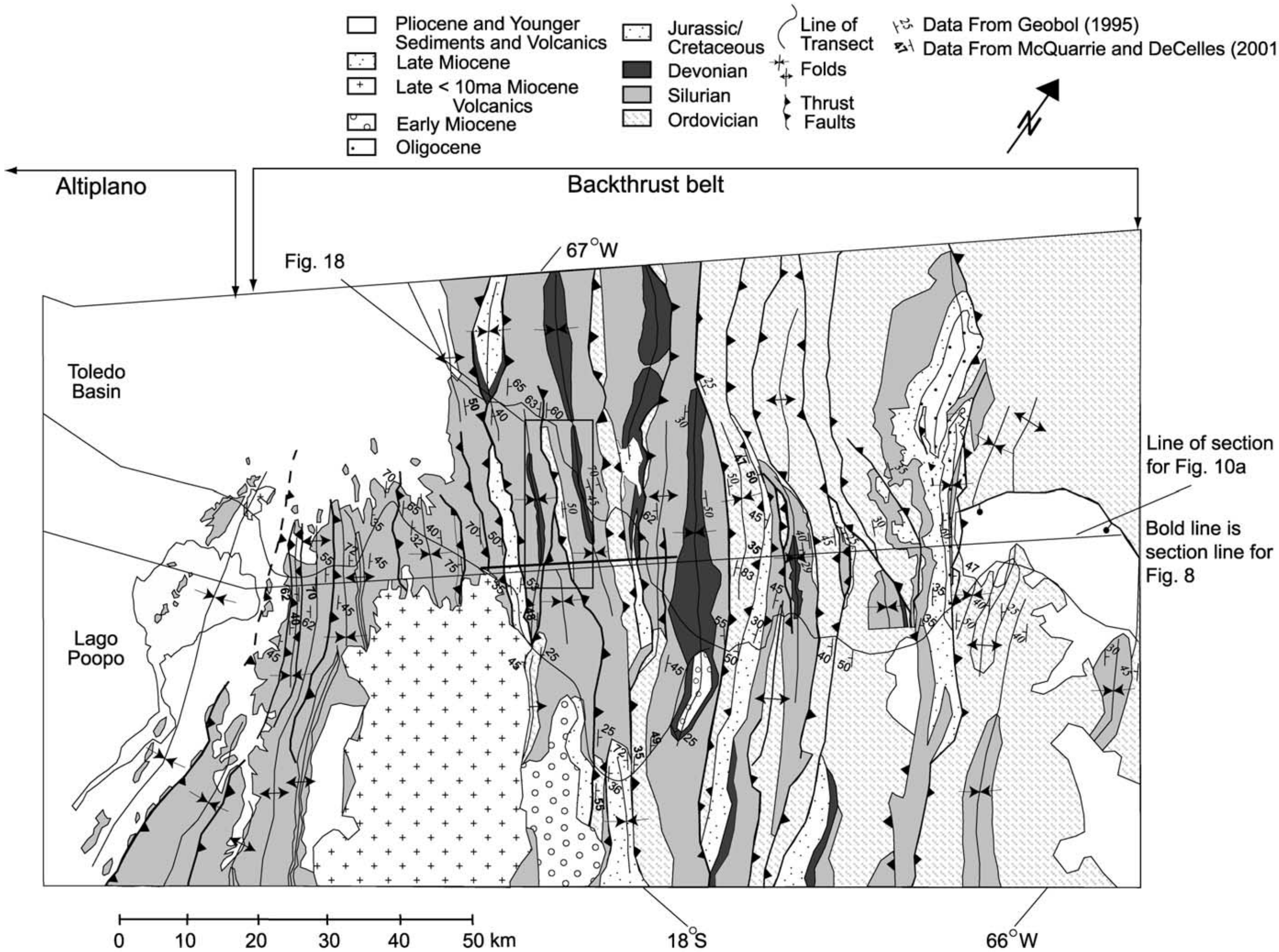

Fig. 2. Geologic map of the central sector of the Central Andean backthrust belt (simplified from Geobol (1995) and modified from McQuarrie and DeCelles (2001)).

fold–thrust belt. This broad area of high elevation (greater that 3 km), internally drained basins and moderate relief has been defined as the central Andean plateau (Isacks, 1988; Gubbels et al., 1993; Masek et al., 1994; Lamb and Hoke, 1997). The central Andean plateau contains three physiographically distinct provinces; the Western Cordillera, an active volcanic arc straddling the international border between Bolivia and Chile, the Altiplano, a wide (200 km) internally drained region of subdued topography east of the Western Cordillera, and the high peaks of the Eastern Cordillera, which reach elevations of ~6.4 km. Deformation within the Eastern Cordillera is bivergent with the west-verging section of the Andean fold–thrust belt on the western side and the east-verging section on the eastern side (Fig. 1b). Elevations drop dramatically from the eastern edge of the Eastern Cordillera to the Subandean zone, which is presently the actively deforming portion of the fold–thrust belt (Fig. 1a).

Two of the key questions still unanswered for this region are how the Andean fold-thrust belt developed with time to create the central Andean Plateau? And, is shortening within the Andean fold–thrust belt sufficient to account for the 70-km-thick (Beck et al., 1996) Andean plateau? These two questions remain unanswered because existing shortening estimates and balanced cross-sections typically consider only the eastern half of the Andes, which are the Eastern Cordillera and Sub-Andean portions of the fold–thrust belt (Kley and Monaldi, 1998) or only schematically link deformation in the hinterland to the foreland (Sheffels, 1990; Lamb and Hoke, 1997; Kley and Monaldi, 1998). Recent studies of the Andean hinterland (McQuarrie and DeCelles, 2001) emphasize the importance of an extensive west-vergent thrust system in the hinterland of the Andean fold–thrust belt and show that through the development of this backthrust belt, 100 km of shortening can be added to previous estimates. The outcrop-scale structures discussed in this paper increase the growing amount of shortening recognized in the central Andean fold-and-thrust belt by adding strain estimates unaccounted for by regional balanced cross-sections.

Table 1
Table of mechanical stratigraphy for the hinterland of the central Andean fold–thrust belt

Age	Formation names	Thickness	Lithologies	Characterization	Outcrop-scale structures
Tertiary	Bolivar, Morochata. Santa Lucia	~ 2–3 km (locally)	Sandstone, siltstone, shale and conglomerates	Stiff	NA
Cret.	El Molino, Chaunaca, Aroifilla	250–1000 m	Sandstones, shales and limestones (thinly bedded)	Soft	NA
Jurassic	Ravelo	< 500 m	Medium-thick bedded, cross stratified sandstone	Stiff	Deformation bands, faults and flexural slip surfaces
Devonian	Belen	< 300 m	Thinly bedded shale and siltstone, rare thin sandstone beds	Soft	Tight intraformational folds, axial planar and bedding planar cleavage
	Vila Vila	650–800 m	Medium to thickly bedded sandstone, common shale to siltstone interbeds	Stiff	Late-stage, low-angle faults, buckling
Silurian	Catavi	500–1700 m	Flaggy sandstone with interbeds of siltstone and shale	Moderately stiff	Flexural slip, décollements, upright and overturned folds, axial planar and bedding planar cleavage, crystal fiber veins, boudins, late-stage, low-angle faults
	Uncia	1000–1800 m	Interbedded siltstone and shale	Soft	Pencil structures, upright and overturned folds, axial planar and bedding planar cleavage, kink bands, late-stage, low-angle faults
	Llallagua	0–1500 m	Medium bedded sandstone, and quartzite with common shale to siltstone interbeds increasing up section	Stiff	Flexural slip, upright and overturned folds, axial planar and bedding planar cleavage, crystal fiber veins, boudins
	Cancaniri	200–600 m	Massive siltstone with uncommon beds of sandstone and siltstone	Soft	Boxwork veins, cleavage
Ordovician	San Benito	↑	Thick bedded quartzite	Stiff	Joints, thrust faults, breccia, crystal fibers, folds en échelon gashes
	Anzaldo	5–7 km	Sandstone with interbeds of siltstone and rare shale	Stiff–soft	Crenulation cleavage, stained worm burrows, pencil cleavage, upright to overturned folds, steeply plunging folds
	Capinota	↓	Interbedded siltstone and shale	Soft–stiff	Pencils, axial planar cleavage and folds

2.2. The central Andean backthrust belt

The area of focus for this study is within the central Andean backthrust belt, a west-verging thrust system located in the hinterland of the eastward-propagating Andean fold–thrust belt (Roeder, 1988; Baby et al., 1990, 1997; Sempere et al., 1990; Roeder and Chamberlain, 1995; McQuarrie and DeCelles, 2001) (Fig. 1b). Although doubly verging orogens are common in the geologic record, with the axis of symmetry typically centered on the suture zone or the volcanic arc (e.g. Beaumont and Quinlan, 1994), the central Andes are unique in that the back-arc fold–thrust belt is also a strongly bivergent system. The west-verging thrust system (the central Andean backthrust belt) has an along-strike length of >600 km and an across-strike width of ~150–200 km (Fig. 1). It is dominated by tight folds (wavelengths of 5–10 km) and steep (45–65°), generally eastward-dipping thrust faults with 5–40 km of displacement (Figs. 1b and 2). The faults throughout the backthrust belt commonly breach the shared limbs of folds placing hanging wall anticlines over footwall synclines, suggesting these structures are fault propagation folds where detachment folding precedes faulting (McNaught and Mitra, 1993; Rait and Dixon, 1997; Wallace and Homza, 1997). Other important structures include imbricate fans, and duplexes (McQuarrie and DeCelles, 2001).

The axes of many of the synclines within the backthrust belt are cored with Jurassic age rock and the common regional elevation of many of the Jurassic-cored synclines suggests a relatively shallow and uniform detachment horizon across the entire width (Fig. 2). In order to keep a relatively shallow and uniform detachment horizon, and because the oldest rocks exposed in the backthrust belt are in the Ordovician Anzaldo Formation, the main detachment level for the west-verging fold–thrust belt is proposed to be within the lower Ordovician shale. Regional cross-sections across the backthrust belt are described in detail in McQuarrie and DeCelles (2001). For the purposes of this paper, the central cross-section (Figs. 1b and 2) is used to connect the several scales of strain.

3. Mechanical stratigraphy

We begin with describing the 'mechanical stratigraphy' of the rock column within the hinterland of the central Andean fold–thrust belt. Our inference about the relative strengths of the various stratigraphic units are based on observable strain at the outcrop level and generally known strength attributes of different rock types (e.g. Jaeger and Cook, 1979). The rocks involved in this hinterland deformation range from Ordovician marine siliciclastic rocks to Tertiary synorogenic sedimentary rocks. The mechanical stratigraphy is summarized in Table 1.

The lowermost Ordovician Capinota Formation contains dark siltite, phyllite, and slate with horizons of sandstone/quartzite near the top of the formation. It is a mechanically weak layer and is interpreted to be a major detachment horizon within the fold–thrust belt. The Capinota Formation grades upward into the interbedded green/brown siltstone and sandstone of the Anzaldo Formation. Overall the Anzaldo Formation acts as a mechanically strong layer with interbedded weak layers. The thick-bedded quartzite of the San Benito Formation is the mechanically strongest layer within the Ordovician sequence. Total exposed thickness of these formations range from 5 to 7 km (Rivas, 1971; Rodrigo-Gainza and Castaños, 1978). Although all three formations are competent, thin beds and alternating sandstone and siltstone permit intraformational deformation through flexural slip.

The Ordovician rocks are conformably overlain by the Silurian Cancañiri Formation (Sempere et al., 1991; Sempere, 1995), which is a mechanically weak diamictite and sandy mudstone that facilitates detachment surfaces within the backthrust belt. It in turn is overlain by the Llallagua Formation, a resistant, and mechanically strong unit of fine-grained sandstone and quartzite with subordinate mudstone. Overlying the Llallagua, is the Silurian Uncia and Catavi Formations. The Uncia Formation is a thick but weak unit composed of shale and siltstone (González et al., 1996). The Catavi Formation contains alternating shale and sandstone beds (González et al., 1996), which accommodate internal deformation as reflected by the presence of outcrop-scale folds, differential thickening and thinning, and secondary detachments.

The Devonian rocks exposed through this portion of the fold–thrust belt are the mechanically strong sandstone and subordinate shale and siltstone of the Vila Vila/Santa Rosa Formation (González et al., 1996). Thin remnants of the Belén/Icla Formation, shale, siltstone and thin (10–20 cm) sandstone beds (González et al., 1996), cap the Vila Vila/Santa Rosa Formation. Jurassic and younger rocks are preserved in the cores of elongate synclines throughout this region of the hinterland. The mechanically stiff Jurassic rocks consist of eolianites and fluvial sandstones (the Ravelo Formation) overlain by conglomerates and siltstones of the Condo and Tarapaya Formations. The Cretaceous units are the Aroifilla, Chaunaca, and El Molino Formations. These formations contain mudstone, siltstone and thin beds of sandstone and are discontinuous throughout this part of the fold–thrust belt with maximum thicknesses less than 500 m. The Cretaceous rocks are overlain by a >10-km-thick sequence of Tertiary synorogenic sedimentary rocks within the Altiplano. Scattered synclines containing Tertiary synorogenic sedimentary rocks throughout the Eastern Cordillera suggest that a 2–3-km-thick foreland basin most likely preceded the fold–thrust belt in this area (Horton 1998; Horton et al., 2001).

Because Andean deformation is most readily defined by the involvement of Jurassic and younger rocks, it is important to understand the regional stratigraphic patterns through the central Andean fold–thrust belt. Throughout the study area (18–17° S), Jurassic rocks generally rest conformably on lower Devonian rocks within the Eastern Cordillera and progressively younger Paleozoic rocks both to the east and west of the crest of the Eastern Cordillera. The presence of deformed Jurassic rocks throughout the study area, and their spatial correlation to the outcrop-scale structures described below implies that small-scale structures are indeed Andean. Outcrop-scale structures are concentrated in hanging wall anticlines and their associated faults, which are commonly adjacent to footwall synclines containing Jurassic rocks. That Jurassic rocks are always confined to footwall synclines, argues strongly against reactivation of earlier normal faults (e.g. Martinez, 1980), which would raise Jurassic and younger hanging wall rocks with respect to the Paleozoic footwall rocks (Welsink et al., 1995).

4. Characterization of outcrop-scale deformation

Across this transect of the Andean fold–thrust belt, domains with large strains (characterized by pervasive outcrop-scale folding and faulting) are separated by wide panels of relatively unstrained, homoclinally dipping strata interpreted to be the limbs of regional-scale folds or flats. High strain domains within the fold–thrust belt are consistently associated with surface breaking faults, the cores of folds, or blind thrusts. The presence of these high strain domains affects the portrayals of structural relations within the cross-section. In particular, the high strain domains provide a mechanism to

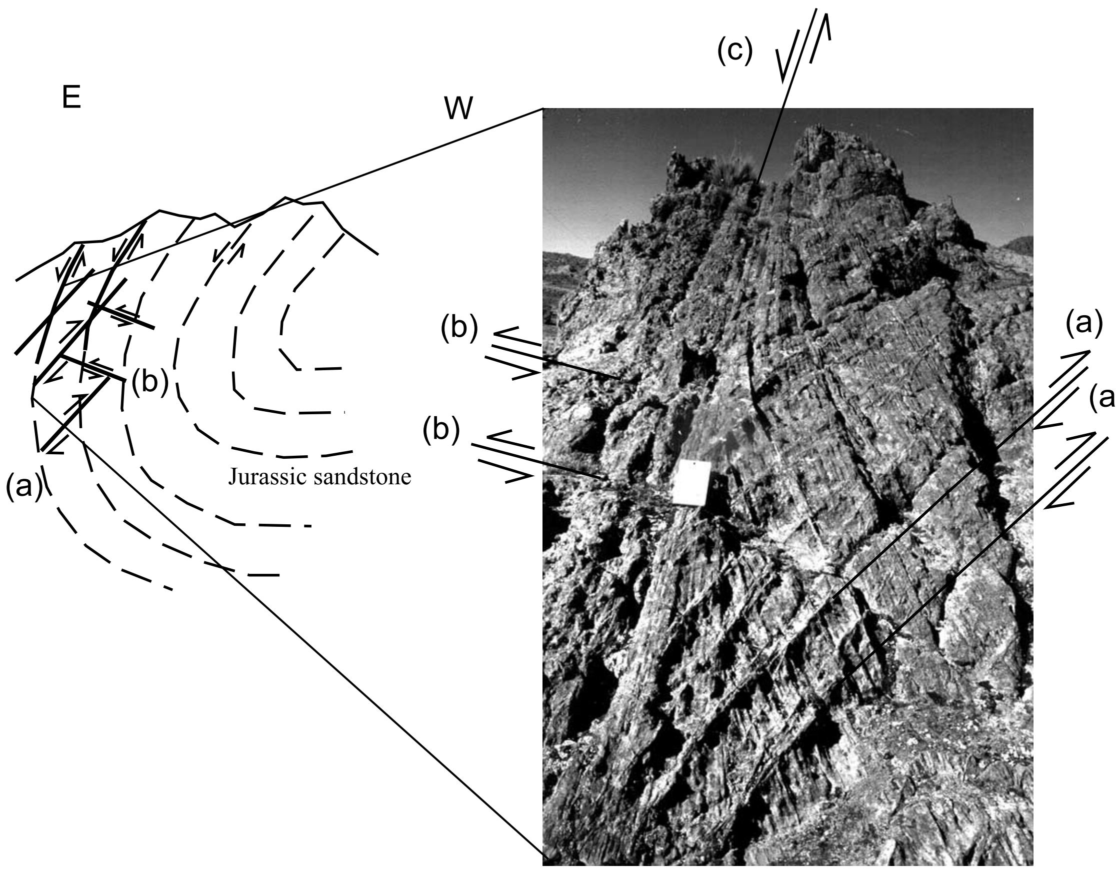

Fig. 3. Photograph and line sketch of out of the syncline slip as facilitated by deformation banding in porous Jurassic sandstone. The photograph and sketch illustrate the geometry of the deformation bands, with the main deformation band being bedding parallel and steeply dipping to the east (c). Other bands dip less steeply and accommodate westward thrusting (a) or are almost horizontal and accommodate eastward thrust displacement (b). Where offsets are visible, the east and west directed deformation bands mutually offset each other. A field notebook for scale is balanced on an east-directed deformation band. The photograph is looking south at the overturned limb of a west-verging syncline.

thicken the hinge zones transforming ordinary concentric (class 1b) folds into quasi-similar (class 1c) folds (Ramsay, 1967; Ramsay and Huber, 1987). This thickening is achieved by the processes discussed in Sections 4.1–4.5.

4.1. Flexural-slip folding

Flexural-slip creates upright or slightly inclined non- to gently plunging folds in the region of study. In the mechanically stiff Jurassic sandstones, this process is achieved through S_0-parallel deformation bands. The deformation bands appear to be braided in map view; however, deformation-band orientations stay mostly parallel with S_0 or along cross-beds and range between N–S and N 35W with almost perpendicular (80–85°) slickenline rakes. The S_0 parallel deformation bands facilitate out of the syncline slip as illustrated in Fig. 3. The strain accomplishing mechanism in the porous Jurassic sandstone is almost always deformation banding (e.g. Davis, 2000). Thus the deformation banding in Fig. 3 reflects both out of the syncline slip and west-verging thrust displacement due to a large west-verging fault on the eastern side of the Jurassic syncline (Fig. 2). Bedding-plane, flexural-slip is also recorded in other formations such as the alternating sandstone and shale of the Catavi Formation (Fig. 4a). This bedding-parallel slip creates flexural-slip slickenlines that are also nearly perpendicular to strike.

4.2. Fold flattening

As deformation increases in front of the propagating fault tip, the interformational folds and perhaps the fault propagation fold itself, begin to flatten. Fold flattening is achieved by incipient development of axial-planar cleavage in argillite (revealed by pencil structures) and pressure solution. Released quartz (or calcite) is then precipitated in gash veins or along joint faces. Axial-planar cleavage and pencil structures are present in very attenuated folds, such as those developed in the siltstone of the Anzaldo Formation (Fig. 4b). They are also found in the broad open folds of the Capinota Formation. The presence of pencil structures suggests 9–26% more strain than can be accounted for by simple line length balancing (Reks and Grey, 1982). Sandstone formations with shale interbeds such as the Catavi Formation or the Llallagua Formation display axial-planar cleavage in upright, tight to isoclinal folds indicating thinning by flattening and pressure dissolution.

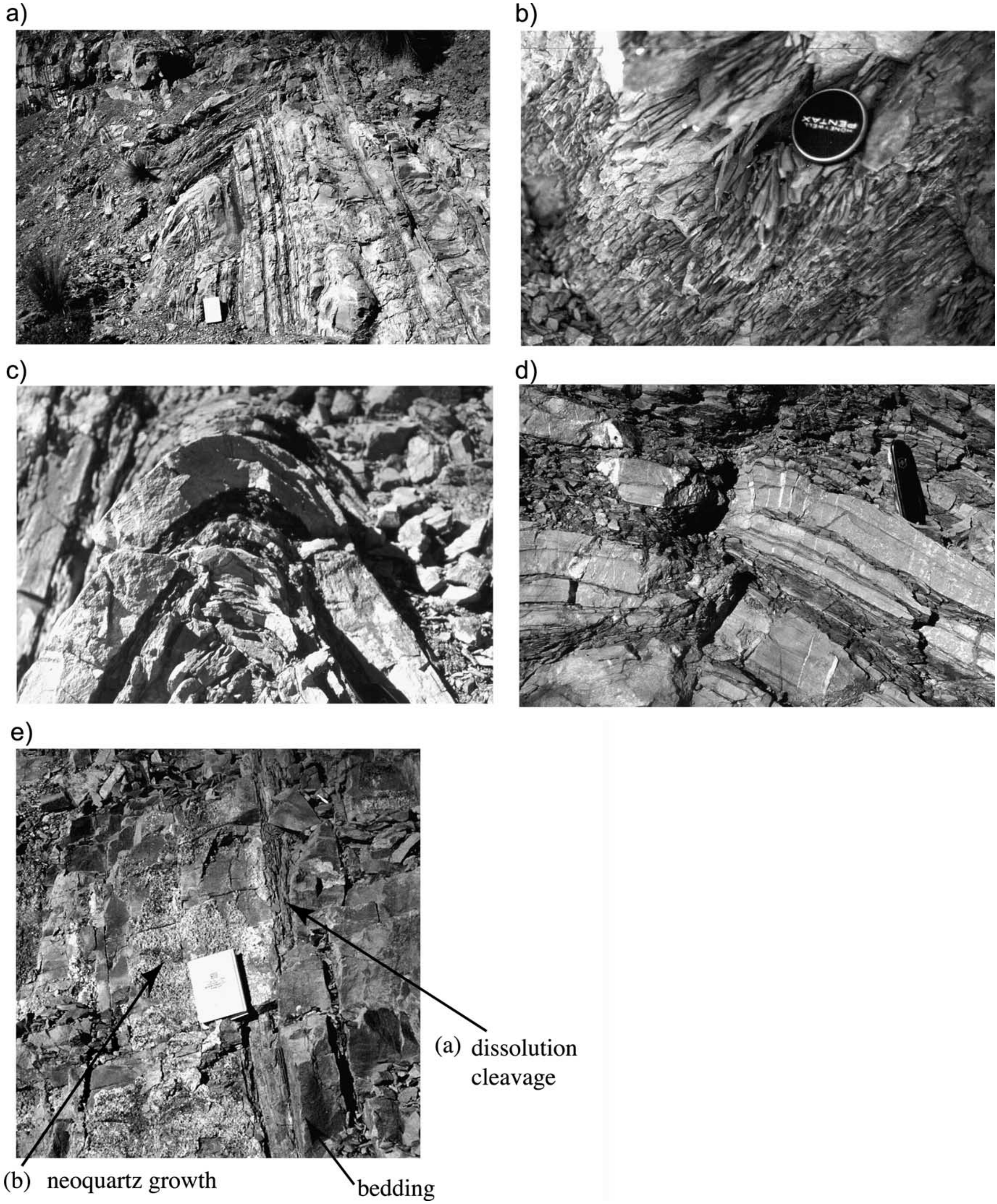

Fig. 4. (a) Photograph of flexural slip folding in the Silurian Catavi Formation. The angle of the photo and the sun make the fold appear discontinuous; however, individual beds can be traced through the axis of the syncline. A field notebook placed at the bottom center is for scale. (b) Photograph of pencil structures within the Anzaldo Formation. The orientation of the pencils mimic the axis of the fold and are Andean (N20°W to N45°W) in their orientations. (c) and (d) Photograph of a fold hinge showing both thickening of shale interbeds within the fold hinge (c) and neoquartz-filled tension gashes on the outer arc of a fold (d). Axial-planar cleavage and pressure solution are well developed in the weaker (darker) shale beds. A 9 cm Swiss knife is the scale in (d), both pictures are at approximately the same scale. (e) Photograph showing the result of concomitant thinning of weak shale interbeds by pressure dissolution (a) and the precipitation of released quartz in the form of crystal-fiber veins on bedding perpendicular joints (b). Field notebook for scale rests on a crystal-fiber vein that is parallel to the plane of the photograph.

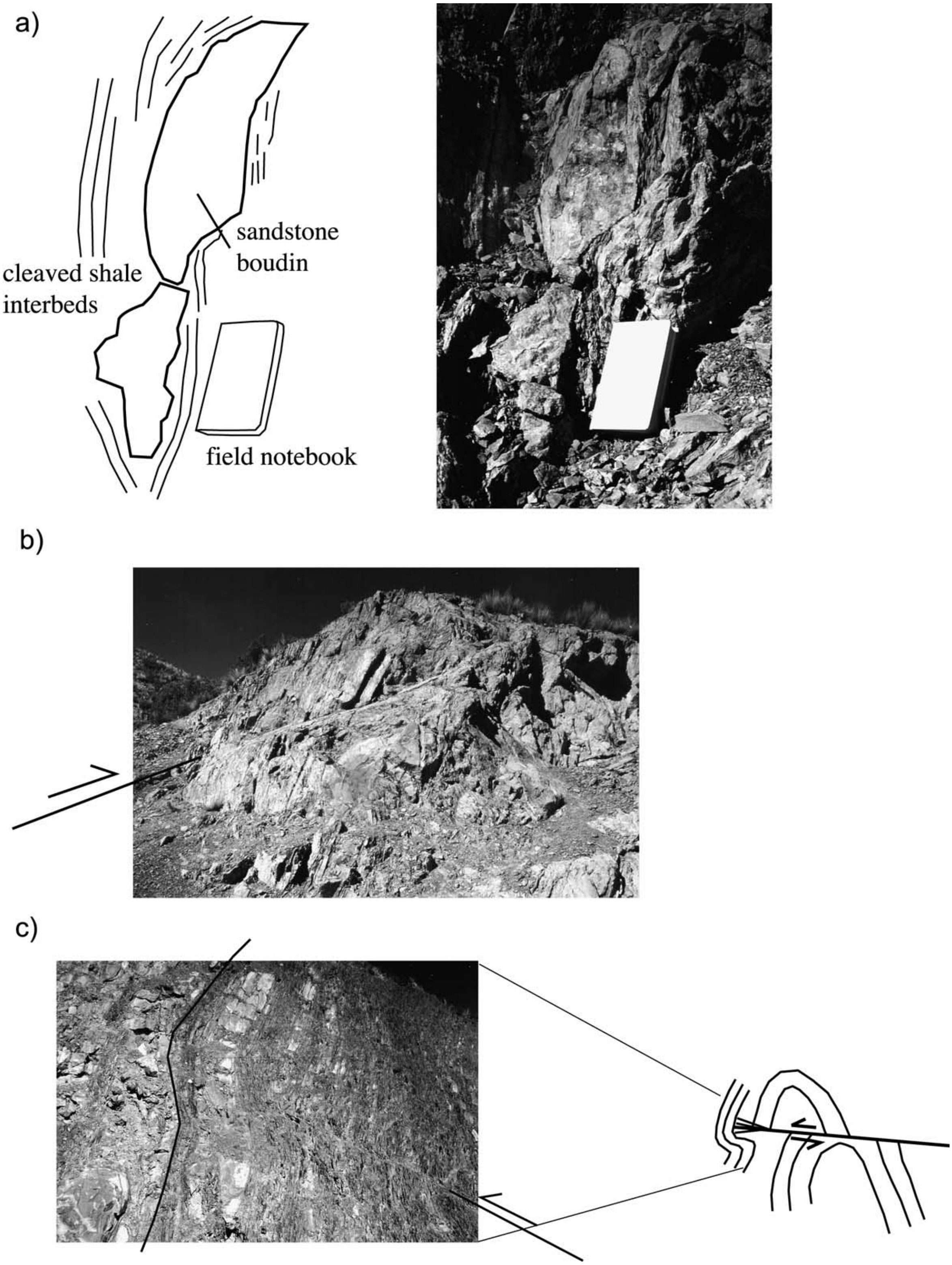

Fig. 5. (a) Sandstone boudins within the Catavi Formation. Field notebook for scale. (b) Late-stage, low-angle fault that displaces the hinge of an outcrop fold. (c) Photograph and line drawing of a tip zone for a late-stage fault. The tip zones of the late-stage, low-angle faults are commonly areas of overturned or refolded folds.

The excess material is displaced to the fold hinges either through the thickening of hinges with pervasively deformed shale or by the precipitation of quartz in crystal-fiber veins on the outer extended portion of the hinge (Fig. 4c and d), or to other (bedding perpendicular) joint surfaces. Fig. 4e shows an example of concomitant pressure solution and formation of crystal-fiber veins. The veins form in bedding-perpendicular joints developed in thick sandstone beds. Clayey siltstone became cleaved and dissolved quartz was precipitated in veins. The slickenlines on the surfaces of these sandstones are also perpendicular to fold axis suggesting flexural slip.

Vertical stretching of the folds during flattening is achieved by boudinage and late-stage, low-angle thrust faults. Especially in alternating sandstone and shale formations, the sandstone layers show strong attenuation in the form of boudins, the spaces between the boudins filled in with the weaker shale beds or precipitated quartz (Fig. 5a).

4.3. Late stage vertical stretching

The last increment of elongation is low-angle (in some cases almost horizontal) thrust faulting that displaces the hinges of folds (Fig. 5b and c). This faulting may also cause refolding or overturned folds at the tip zones of the faults (Fig. 5c) as noted in the Pennsylvanian Valley and Ridge province by Nickelsen (1986) and Gray and Mitra (1993). The planar nature of the faults indicates they occur very late in the development of the deformation.

4.4. Latest stage kinking

Late stage kinking occurred in steeply dipping layers after flexural slip along bedding has been reduced by the tightening of the folds. The kink bands are 30–45-cm-thick with interlimb angles of 90°. The bands themselves tip out on the outcrop scale (20 m vertical) (Fig. 6a). We have used the changes in the kink band geometry along dip as a proxy of how the band developed through time. The tip zone is narrow, and the dips of the strata within this zone are less steep (interlimb angles >90°) than where the band is well developed towards the base of the outcrop. We interpret this to indicate that the kink band has widened and that the bedding within the band has progressively rotated through time to accommodate layer parallel shortening. Based on studies that propose that kink bands widen with increasing deformation (Weiss, 1980; Stewart and Alvarez, 1991), the size of the kink bands, their narrow breadth and finite length, indicate they formed at a late stage.

In the same way that unfolded kink bands reflect late stage development, the unfolded form of the low-angle, small-offset faults suggests they are also late. Both of these brittle, late-stage features continuously created a simultaneous horizontal shortening and vertical stretching of the deformed rocks.

4.5. Large-offset faults

Due to the erodable nature of most fault zones, large faults are seen where two competent units are juxtaposed along thin zones of failure. An example is a fault that places the mechanically strong Anzaldo Formation over the quartzite of the San Benito Formation (Fig. 6b and c). The main fault is confined to a 10-cm-thick gouge zone. However, the zone of deformation extends into both the overlying and underlying formations. The footwall San Benito Formation is deformed by small, intraformational faults forming a duplex. Where the horses join the main fault, the bedrock is saturated with closely spaced cleavage (Fig. 6c) most likely due to a lack of accommodation space (Marshak and Engelder, 1985). In this same zone of duplexing, the overlying Anzaldo Formation deformed in a series of small-displacement backthrusts that are listric to the main fault (Fig. 6b–d).

4.6. Development of outcrop-scale structures

The development of these outcrop-scale structures is schematically displayed in Fig. 7. The main detachment fault propagates outward on a regional flat or detachment level. If the propagation to slip ratio is low, slip and strain associated with this detachment fault (McNaught and Mitra, 1993), especially as it begins to propagate upward (Suppe, 1983; Mitra, 1990), is accommodated by folding in front of the fault tip (McNaught and Mitra, 1993). We define this area in front of the fault tip that accommodates the transition from the slipped region to the unslipped region, as the process zone of a propagating fault tip. In the process zone, within the regional fold and above the propagating fault tip, intraformational folds form through flexural slip folding. This layer parallel shear imparts a fissility to the less competent units and is expressed as bedding-parallel slickenlines in the more competent units. As both the regional and intraformational folding increase, the folds begin to flatten through cleavage development and elongate vertically through boudinage and late-stage, low-angle thrust faults. Once the detachment fold has developed, the thrust can take advantage of the weak, thickened core as a place to cut up-section, creating the hanging wall anticline, footwall syncline pair (McNaught and Mitra, 1993) seen in the map pattern of the backthrust belt (Fig. 2). Within the strained zones there is a progression from (1) coaxial strain that is expressed as flexural slip folding and buckling of beds to (2) flattening with negative dilation (thus no vertical stretching) through the formation of axial-planar cleavage, to finally (3) vertical stretching in conjunction with shortening achieved by layer thinning processes (boudinage, late-stage thrust faults) (Fig. 7). Similar progressive strain has been documented within other fold–thrusts belts (Mitra et al., 1984; Mitra, 1987; Boyer and Mitra, 1988; Gray, 1991; Gray and Mitra, 1993; Rait and Dixon, 1997), although constraints such as temperature, pressure and strain rate

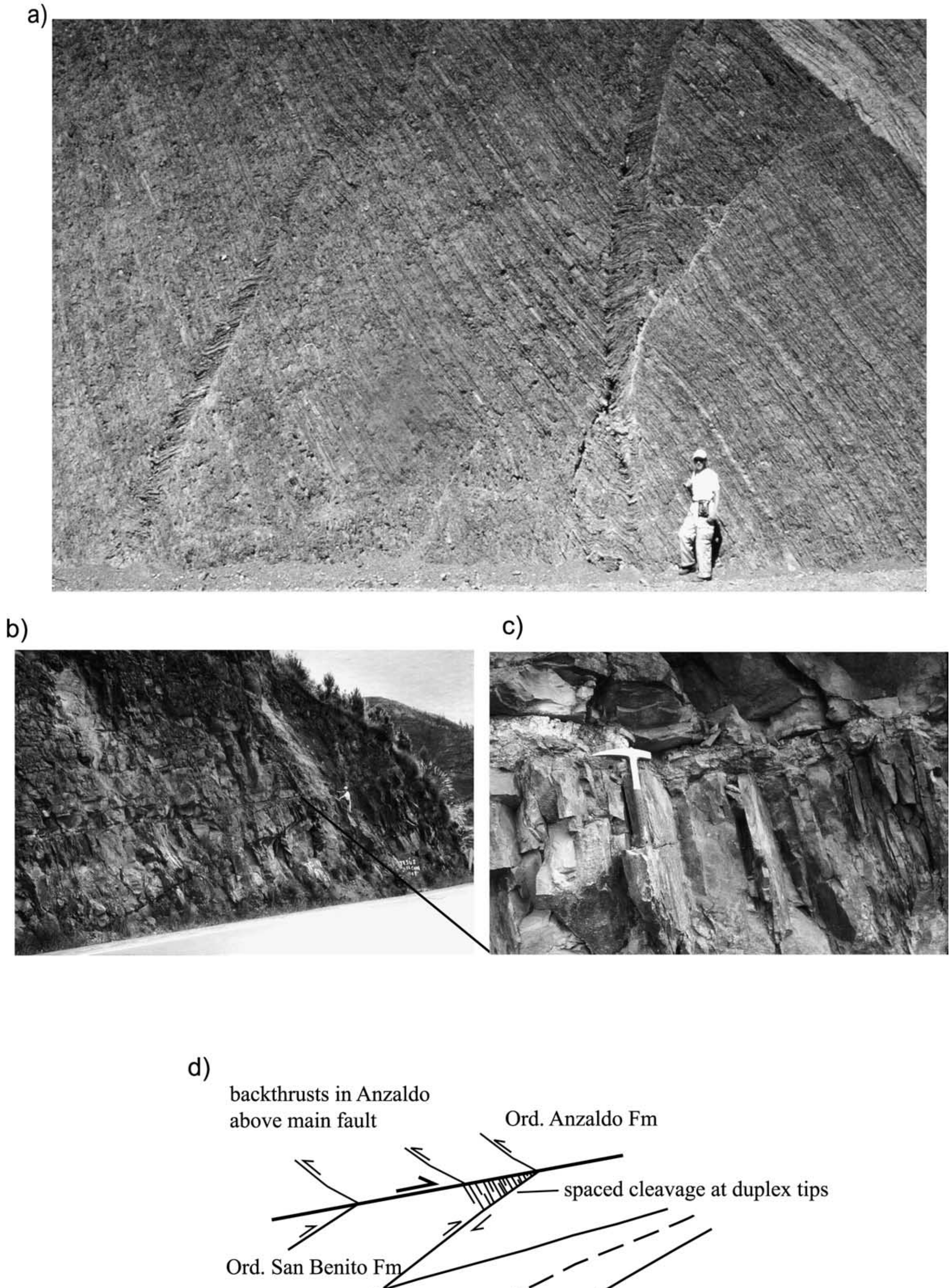

Fig. 6. (a) Outcrop exposure of kink bands. The kink bands are widest at their base and tip out towards the top of the exposure. Note the change in both width and interlimb angle of the kink bands along dip. (b) Large offset fault placing an Ordovician Anzaldo flat on an Ordovician San Benito flat. A Geologist is perched on the subhorizontal fault plane on the far right side. The prominent plane dipping 30° to the left (NW) is a small intraformational duplex within the San Benito Formation. (c) Photograph of gouge zone and joint saturated tip zone with hammer for scale. The upper bound for the joints is the main fault. (d) Line drawing of large offset fault showing types of associated structures. These include backthrusts within the overlying Anzaldo Formation, intraformational duplexes in the San Benito formation and joint saturation at the branch points of the duplexes.

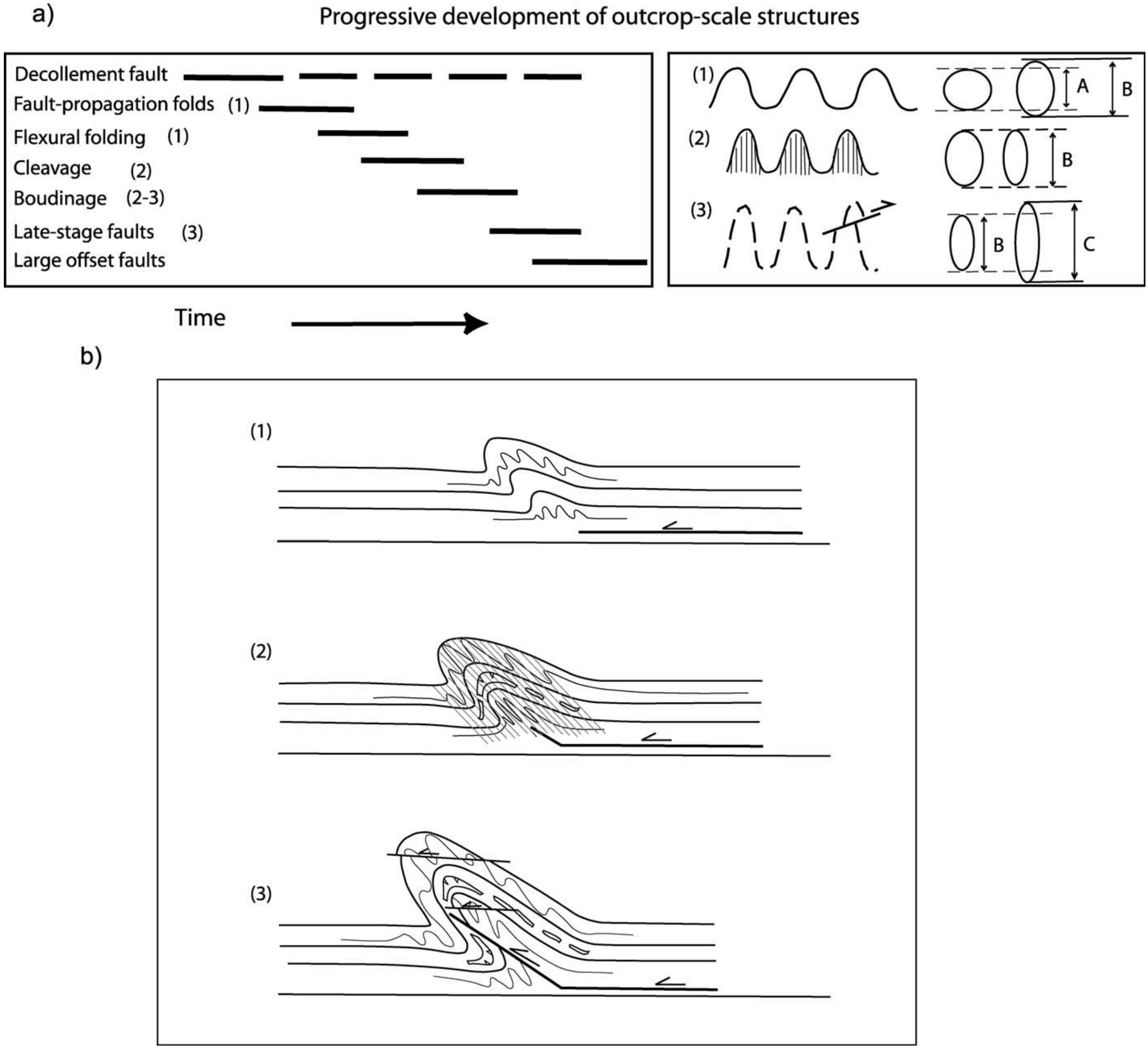

Fig. 7. (a) Chart displaying the progressive development of the outcrop-scale structures. Bracketed numbers refer to the mechanisms of strain discussed in the text: (1) co-axial strain or pure shear, (2) flattening with negative dilation (thus no vertical stretching), and (3) vertical stretching in conjunction with shortening. (b) Schematic development of fault-propagation fold and associated intraformational deformation. Numbers (1–3) correspond to strain mechanisms listed above.

add a variability of deformation mechanisms and resulting micro- to outcrop-scale structures (Mitra, 1987).

5. Linking the scales of strain

The deformation style expressed by all of these mechanisms is one that created horizontal shortening via flexural-slip folding and limb thinning, axial-planar pressure solution. Vertical stretching was accommodated by the development of boudinage and tightening of the fold hinge and finally late-stage decapitation of the fold hinge by low-angle faults. We propose this shortening and thickening occurs in the process zone in front of a propagating fault tip. Fig. 8 shows the distribution of strain domains for a swath of structures in the backthrust belt. The basic fold–thrust belt mechanism evident in the cross-section is fault-propagation folding.

The map patterns of the backthrust belt show a mixture of tight wavelength folds cut by predominantly west-verging faults in Ordovician through Cretaceous rocks (Fig. 2). Stratigraphic separation across these faults is greatest in the center of a given fault trace and decreases gradually until the fault tips out in a plunging anticline. Downplunge

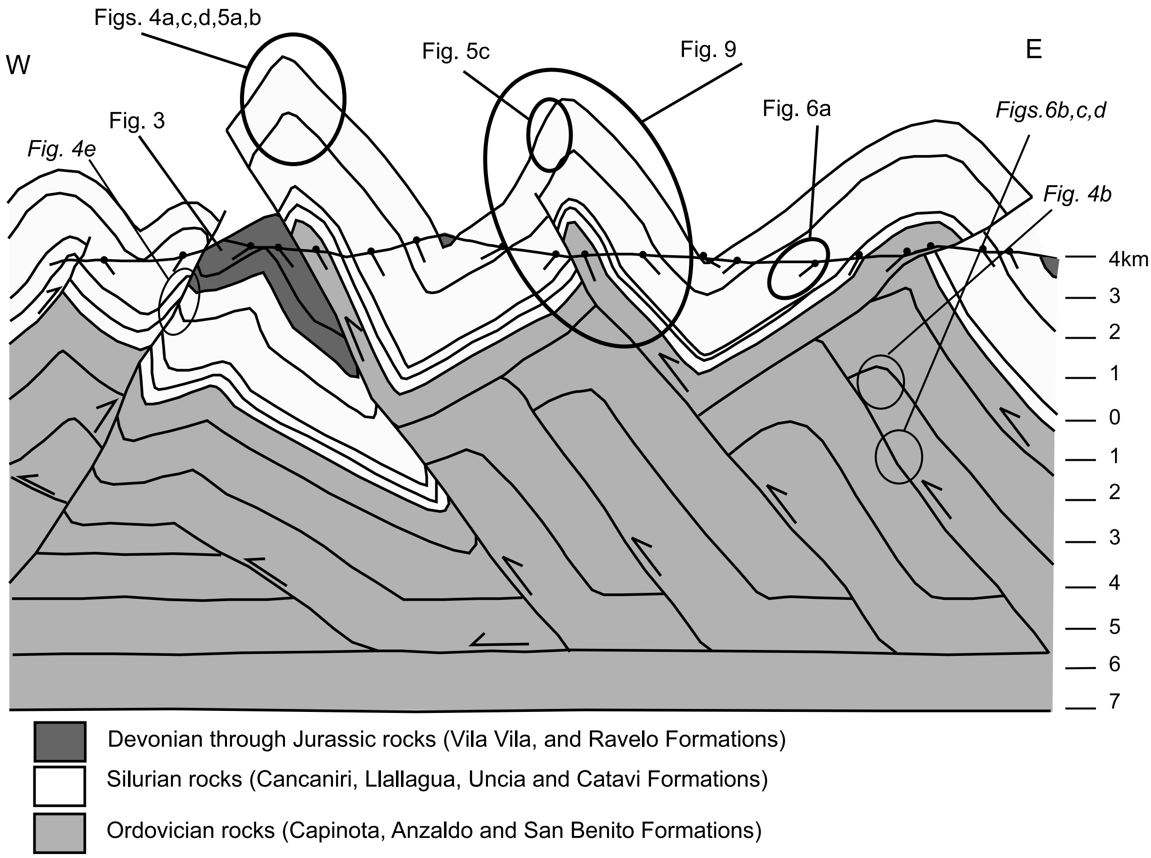

Fig. 8. Distribution of high strain domains discussed in this paper with respect to the regional structures in the central Andean backthrust belt (see Figs. 2 and 10 for location). The cross-section is drawn with no vertical exaggeration. The outcrop-scale structures discussed in the text and shown in the previous figures are referenced to their locations in the fold–thrust belt as circled regions. Figures in the line of section are circled with bold lines. Thinner circles and italic numbers indicate figures from off the line of section but in correlative positions. The outcrop-scale structures emphasized in this paper are concentrated in the hinges or the immediate fault zone of fault-propagation folds and are separated by long panels of homogeneously dipping strata.

viewing of the map pattern from one faulted fold (Fig. 9), especially towards the tip of the fault, shows the regional-scale geometries of the fault propagation folds. The presence of a syncline within the footwall of a fault-propagation fold and large amplitude anticline at the thrust tip suggest that the fold preceded rather than accompanied thrust propagation (McNaught and Mitra, 1993; Rait and Dixon, 1997; Wallace and Homza, 1997). This sequential development of folding and deformation in the process zone preceding the fault is also supported by the progressive development of the outcrop-scale structures.

The steep dips of many faults within the Eastern Cordillera have been used as arguments for the low shortening of this part of the fold–thrust belt (e.g. Martinez, 1980). Sheffels (1990) suggested that the repeated juxtaposition of steep stratigraphic units across these faults requires that the dips of the faults flatten with depth, thus dramatically increasing the shortening accommodated by an individual fault. Field data confirm that faults in the Eastern Cordillera cut steeply up-dip as depicted on maps, cross-sections, and in restored sections (McQuarrie and DeCelles, 2001). We suggest that the steep dips of most of these faults are owed to the development of fault-propagation folds. As a fault-propagation fold grew in front of the fault tip (McNaught and Mitra, 1993), shortening in these rocks was accomplished first by intense deformation, which tightened and localized the deformation creating a zone of weakness (McNaught and Mitra, 1993), and later by faulting that cut up steeply with respect to bedding orientations.

Seismic data are concentrated within the Altiplano basin and reveal the transition between the central Andean backthrust belt in the western portion of the Eastern Cordillera and the Altiplano (McQuarrie and DeCelles, 2001). Where the Paleozoic rocks are imaged on the seismic lines, they are shown as a series of steeply (45° +) east-dipping reflectors. This geometry is more compatible with fault-propagation folding, which produces both steeply dipping beds and faults, than the ramp flat geometries in fault-bend folding or the steep faults and flat bed geometries predicted by pure reverse faulting.

Fig. 8 is a local cross-section illustrating the zones of strain described above. The figure magnifies an area within the regional cross-section (Fig. 10) allowing us to cross the boundary between the two scales of strain. The strain domains presented in the first part of this paper are referenced to specific portions of the fold–thrust belt. The

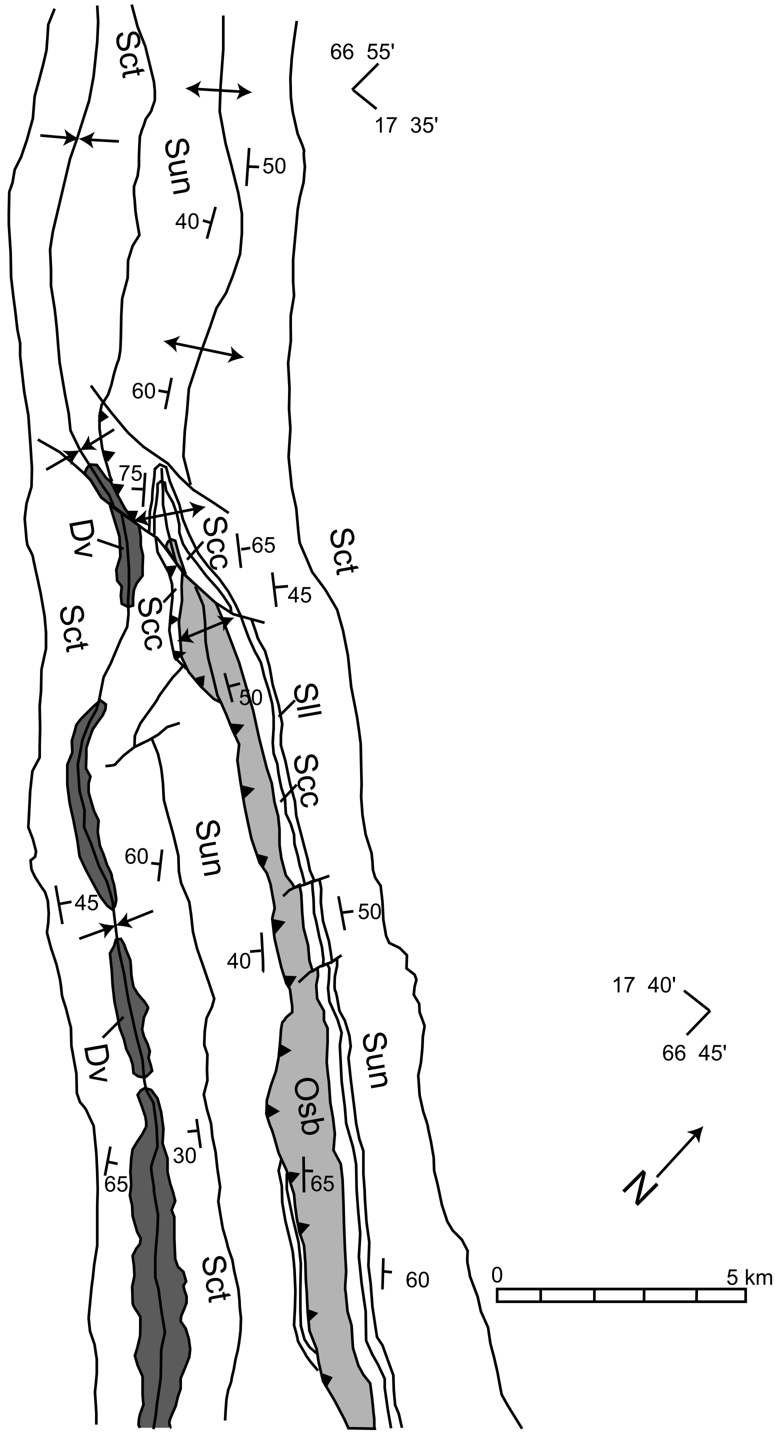

Fig. 9. Map view of a fault-propagation fold simplified from Geobol (1994a,b). Dv—Devonian Vila Vila Formation; Sct, Sun, Sll, Scc—Silurian Catavi, Uncia Llallagua and Cancañiri Formations, respectively; Osb—Ordovician San Benito Formation. The geometry of the structure can be envisioned with a down-plunge view to the north-northwest. The cross-sectional representation of this structure is shown in Fig. 8.

outcrop-scale structures cluster around the faults and the tight folds. Other zones of deformation include the syncline hinges between the fault-propagation folds (Figs. 4b and 8), and late stage kinking and faulting in the undeformed, homoclinally dipping limbs of the folds.

The fault-propagation fold mechanism is observed on two levels. The tight, detached fold train, involving rocks from upper Ordovician to Jurassic, is supported by the short wavelength folds that are expressed on the maps throughout the area (e.g. Geobol, 1995), field observations, and local seismic control. The mapped distribution of rock units forces significant changes in bedding thicknesses, especially thickening in the hinges of folds and thinning on the limbs. Bedding thickness variations suggest that horizontal

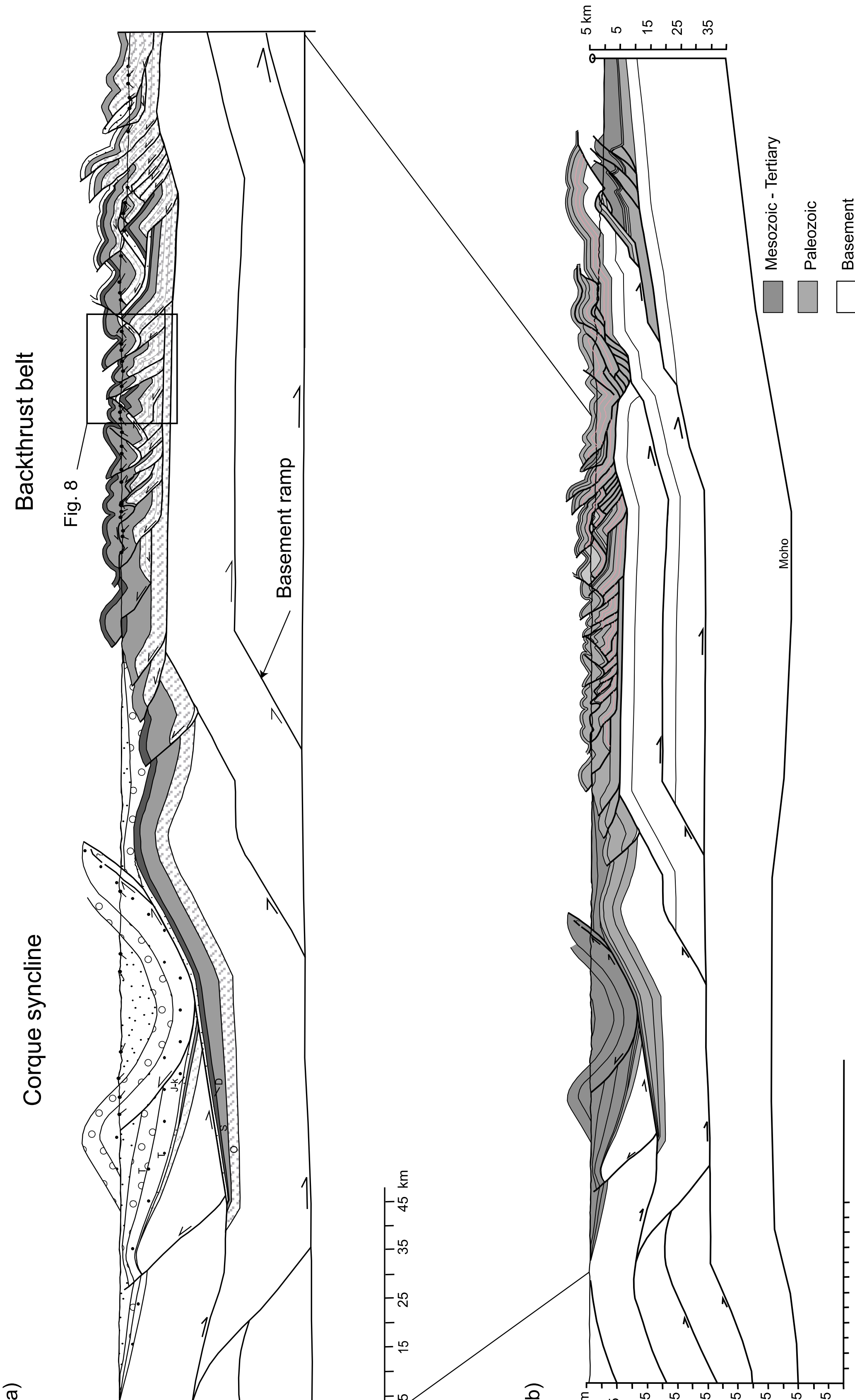

Fig. 10. Regional cross-sections for the central Andean fold–thrust belt (from McQuarrie and DeCelles, 2001). Location of cross-sections is indicated in Figs. 1 and 2. (a) Cross-section through the central Andean backthrust belt. The 12 km step between the level of the Paleozoic rocks within the backthrust belt and the level of the Paleozoic rocks underneath the Altiplano is accommodated by a 12-km-thick basement thrust and ramp that lifts the area of the backthrust belt with respect to the Altiplano. Pattern and shading are the same as in Fig. 2. (b) Regional cross-section for the entire Andean fold-and-thrust belt showing location of the backthrust belt and the extent of the basement thrusts.

shortening and vertical stretching are important in accommodating deformation at the regional scale. This is shown in the cross-section as the evolution of folds from class 1b concentric folds, into quasi-similar, class 1c folds. The deeper level of fault propagation folding and duplexing in the lower Ordovician rocks reflect the need to balance the shortening in the upper levels with that in the lower levels, and to fill space. Map and field observations in the exposed Ordovician rocks to the east suggest that fault propagation folding is a viable deformation mechanism for the unexposed Ordovician (Geobol, 1994b, 1995). This two-tiered fold-and-thrust belt is termed a blind thrust system and is a common form of deformation on other fold–thrust belts (Dunne and Ferrill, 1988).

6. Tectonic scale structures

The strongly deformed, west-verging central Andean backthrust belt (McQuarrie and DeCelles, 2001), places Silurian rocks against a gently deformed, large-amplitude syncline in Tertiary synorogenic sediments of the Altiplano basin (Figs. 1b and 10). In places, the thickness of the syntectonic sediments is greater than 10 km. Minimum depth to basement under the backthrust belt and the Altiplano requires a 12 km step in the elevation of basement between the two provinces. The 12 km offset in the basement is accommodated by a large east-vergent basement thrust, which lifts the Paleozoic section with respect to the Tertiary filled Altiplano (McQuarrie and DeCelles, 2001). The eastward propagation of the basement thrust is accommodated within the Paleozoic cover rocks by the westward propagation of the backthrust belt. Kinematic reconstructions of the Andean fold–thrust belt suggest an early, western fold–thrust belt 'jumped' eastward (200 + km) into the Eastern Cordillera, capturing the Altiplano basin as a crustal-scale piggyback basin, and reducing taper to zero (Fig. 10) (McQuarrie and DeCelles, 2001) The kinematic development of the fold–thrust belt suggests that the backthrust belt developed as a taper-building mechanism after the basement megathrust overextended the system eastward (McQuarrie and DeCelles, 2001). The western propagation of the backthrust belt (Fig. 10) thickened the hinterland allowing the continued eastward propagation of the fold–thrust belt. This taper-building mechanism is expressed even in the outcrop-scale structures of the backthrust belt. These structures show pervasive shortening, vertical elongation and thickening. This process, visible at all scales from outcrop to tectonic, allowed the Andean fold–thrust belt to build thickness (i.e. taper) in the hinterland as a means to continue propagation eastward.

7. Conclusion

The sequential development of outcrop-scale structures is one that supports horizontal shortening and vertical thickening through the development of: (1) flexural-slip folds, (2) axial-planar cleavage, (3) boudinage and late stage faulting, and (4) kink bands. These structures cluster around the discrete faults and the tight propagation folds in the hanging walls and footwalls, and are separated by panels of homoclinally dipping strata as seen on the regional sections. This interdependence of the different scales emphasizes the importance of structures at all scales. The outcrop-scale structures reveal the internal strain patterns consistent with fault-propagation folding, strengthening the portrayal of fault-propagation fold structures on the regional cross-section. Fault-propagation fold constructions permit the accrual of strain, whereas fault-bend fold models generally do not. Fault-bend folding plays a role, but it alone cannot explain the presence of structural domains of intense strain achieved through folding, flattening, and vertical extension, especially in the critical fault boundary zones between domains. The presence of strongly strained domains shows that estimates of shortening based on line length balancing are conservative. Another 10% of shortening could be added based on our estimates of outcrop-scale strain in specific domains coinciding with the presence of exposed thrust faults or presumed blind thrusts. The horizontal shortening and vertical stretching seen at all scales play an important role tectonically as a means of increasing taper in the hinterland, allowing the fold–thrust belt to continue to propagate eastward.

Acknowledgements

This research was supported through a research grant from the National Science Foundation (INT-9907204), American Association of Petroleum Geologists, Geological Society of America, and the University of Arizona Geostructures Partnership. Logistics and access to field sites were provided by Juan Huachani, Sohrab Tawackoli, and Marcelo Claure Zapata of Sergeomin (La Paz). Access to seismic lines was possible through the generosity of Yacimientos Petroleros Fiscales Bolivianos (YPFB), especially Ramberto Quevedo Villagomez and William McKenney (YPFB), and German Saenz Campuzano and Dulfredo Villa Murillo of Prosis. We also thank Gautam Mitra, João Hippertt and an anonymous reviewer for their time and comments.

References

Baby, P., Sempere, T., Oller, J., Barrios, L., Hérail, G., Marocco, R., 1990. A late Oligocene–Miocene intermountain foreland basin in the southern Bolivian Altiplano. Comptes Rendus Académie des Sciences Serie II 311, 341–347.

Baby, P., Rochat, P., Mascle, G., Hérail, G., 1997. Neogene shortening contribution to crustal thickening in the back arc of the Central Andes. Geology 25, 883–886.

Beaumont, C., Quinlan, G., 1994. A geodynamic framework for interpreting crustal-scale seismic reflectivity patterns in compressional orogens. Geophysical Journal International 116, 754–783.

Beck, S.L., Zandt, G., Myers, S.C., Wallace, T.C., Silver, P.G., Drake, L., 1996. Crustal thickness variations in the Central Andes. Geology 25, 407–410.

Boyer, S.E., Mitra, G., 1988. Relations between deformation of crystalline basement and sedimentary cover at the basement/cover transition zone of the Appalachian Blue Ridge Province. In: Mitra, G., Wojtal, S.F. (Eds.), Geometries and Mechanism of Thrusting with Special Reference to the Appalachians, Geological Society of America Special Paper 222, pp. 119–136.

Davis, G.H., 2000. Structural geology of the Southern Utah Parks and Monuments Region, Colorado Plateau, with special emphasis on deformation band shear zones. Geological Society of America Special Paper 342, 158.

Dunne, W.M., Ferrill, D.A., 1988. Blind thrust systems. Geology 16, 33–36.

Geobol (Servicio Geológico de Bolivia), 1994. Carta Geologica de Bolivia: Bolivar (serie 1-CGB-27), scale 1:100,000.

Geobol (Servicio Geológico de Bolivia), 1994. Carta Geologica de Bolivia: Tapacari (serie 1-CGB-24), scale 1:100,000.

Geobol (Servicio Geológico de Bolivia), 1995. Mapas Tematicos de Recursos Minerales de Bolivia: Cochebamba (serie II-MTB-3B), scale 1:250,000.

González, M., Díaz-Martinez, E., Ticlla, L., 1996. Comentarios sobre la estratigraphia del Silurico y Devonico del norte y centro de la Cordillera Oriental y Altiplano de Bolivia. Simposio Sul Americano do Siluro–Devoniano, Ponta Grossa. Anais, 117–130.

Gray, M.B., 1991. Progressive deformation and structural evolution of the southern Anthracite region, Pennsylvania, Ph.D. thesis, University of Rochester, 277pp.

Gray, M.B., Mitra, G., 1993. Migration of deformation fronts during progressive deformation: evidence from detailed structural studies in the Pennsylvanian Anthracite region, USA. Journal of Structural Geology 15, 435–449.

Gubbels, T.L., Isacks, B.L., Farrar, E., 1993. High-level surfaces, plateau uplift, and foreland development, Bolivian central Andes. Geology 21, 695–698.

Horton, B.K., 1998. Sediment accumulation on top of the Andean orogenic wedge: Oligocene to late Miocene basins of the Eastern Cordillera, southern Bolivia. Geological Society of America Bulletin 110, 1174–1192.

Horton, B.K., Hampton, B.A., Waanders, G.L., 2001. Paleogene synorogenic sedimentation in the Altiplano Plateau and implications for initial mountain building in the Central Andes. Geological Society of America Bulletin 113, 1387–1400.

Isacks, B.L., 1988. Uplift of the central Andean plateau and bending of the Bolivian orocline. Journal of Geophysical Research 93, 3211–3231.

Jaeger, J.C., Cook, N.G.W., 1979. Fundamentals of Rock Mechanics. 3rd ed. Chapman and Hall, London, UK.

Kley, J., Monaldi, C.R., 1998. Tectonic shortening of the Andes: how good is the correlation? Geology 26, 723–726.

Lamb, S.H., Hoke, L., 1997. Origin of the high plateau in the Central Andes, Bolivia, South America. Tectonics 16, 623–649.

Marshak, S., Engelder, T., 1985. Development of cleavage in limestone of a fold-thrust belt in eastern New York. Journal of Structural Geology 7, 345–359.

Martinez, C., 1980. Structure et évolution de la chaîne hercynienne et de la chaîne andine dans le nord de la Cordillère des Andes de Bolivie. Mémoire Orstom 119, 352 Paris.

Masek, J.G., Isacks, B.L., Fielding, E.J., 1994. Erosion and tectonics at the margins of continental plateaus. Journal of Geophysical Research 99, 13941–13956.

McNaught, M.A., Mitra, G., 1993. A kinematic model for the origin of footwall synclines. Journal of Structural Geology 15, 805–808.

McQuarrie, N., DeCelles, P.G., 2001. Geometry and structural evolution of the central Andean backthrust belt, Bolivia. Tectonics 20, 669–692.

Mitra, G., Elliott, D., 1980. Deformation of Basement in the Blue Ridge and the development of the South mountain cleavage. In: Wones, D.R. (Ed.), Caledonides in the USA. Department of Geological Sciences Virginia Polytechnical and State University Memoir 2, pp. 307–311.

Mitra, G., Yonkee, W.A., Gentry, D.J., 1984. Solution cleavage and its relationship to major structures in the Idaho–Wyoming–Utah thrust belt. Geology 12, 354–358.

Mitra, S., 1987. Regional variations in deformation mechanisms and structural styles in the central Appalachian orogenic belt. Geological Society of America Bulletin 98, 569–590.

Mitra, S., 1990. Fault-propagation folds: geometry, kinematic evolution, and hydrocarbon traps. American Association of Petroleum Geologists Bulletin 74, 921–945.

Nickelsen, R.P., 1986. Cleavage duplexes in the Marcellus Shale of the Appalachian foreland. Journal of Structural Geology 8, 361–371.

Pareja, J., Vargas, C., Suarez, R., Ballon, R., Carrasco, R., and Vilaroel, C., 1978. Mapa geologico de Bolivia. Memoria Explicativa. Servicio Geologico de Bolivia, 27 pp., La Plaz.

Rait, G.J., Dixon, J.M., 1997. Kinematic evolution of the Canadian Rockies fault-propagation folds. American Association of Petroleum Geologists Annual Meeting Abstracts 6, 95–96.

Ramsay, J.G., 1967. Folding and Fracturing of Rocks. McGraw-Hill, New York.

Ramsay, J.G., Huber, M.I., 1987. The Techniques of Modern Structural Geology, Volume 2: Folds and Fractures. Academic Press, London.

Reks, I.L., Grey, D.R., 1982. Pencil structure and strain in weakly deformed mudstone and siltstone. Journal of Structural Geology 4, 161–176.

Rivas, S., 1971. Ordovicíco del corazón de Bolivia. Boletin Geobol 15, 9–15.

Roeder, D., 1988. Andean-age structure of Eastern Cordillera (province of La Paz, Bolivia). Tectonics 7, 23–39.

Roeder, D., Chamberlain, R.L., 1995. Structural geology of Sub-Andean fold and thrust belt in northwestern Bolivia. In: Tankard, A.J., Suarez, R., Welsink, H.J. (Eds.), Petroleum Basins of South America. American Association of Petroleum Geologists Memoir 62, pp. 459–479.

Rodrigo-Gainza, L.A., Castaños, A., 1978. Sinopsis estratigraphia de Bolivia. I Paleozoico. Academia Nacional de Ciencias de Bolivia, La Paz.

Sempere, T., 1995. Phanerozoic evolution of Bolivia and adjacent regions. In: Tankard, A.J., Suarez, R., Welsink, H.J. (Eds.), Petroleum Basins of South America. American Association of Petroleum Geologists Memoir 62, pp. 207–230.

Sempere, T., Hérail, G., Oller, J., Bonhomme, M.G., 1990. Late Oligocene–early Miocene major tectonic crises and related basins in Bolivia. Geology 18, 946–949.

Sempere, T., Baby, P., Oller, J., Hérail, G., 1991. Calazaya Nappe: evidence for major shortening controlled by paleostructural elements in the Bolivian Andes. Comptes Rendus Académie des Sciences Serie II 312, 77–83.

Sheffels, B.M., 1990. Lower bound on the amount of crustal shortening in the central Bolivian Andes. Geology 23, 812–815.

Stewart, K.G., Alvarez, W., 1991. Mobile-hinge kinking in layered rocks and models. Journal of Structural Geology 13, 243–259.

Suppe, J., 1983. Geometry and kinematics of fault-bend folding. American Journal of Science 283, 684–721.

Wallace, W.K., Homza, T.X., 1997. Differences between fault-propagation folds and detachment folds and their subsurface implications. American Association of Petroleum Geologists Annual Meeting Abstracts 6, 122.

Weiss, L.E., 1980. Nucleation and growth of kink bands. Tectonophysics 65, 1–38.

Welsink, H.J., Martinez, E., Aranibar, O., Jarandilla, J., 1995. Structural inversion of a Cretaceous rift basin, southern Altiplano, Bolivia. In: Tankard, A.J., Suarez, R., Welsink, H.J. (Eds.), Petroleum Basins of South America. American Association of Petroleum Geologists Memoir 62, pp. 305–324.